Energy transfer processes observed in the scintillation decay of BaF_2:La

1992 J. Phys.: Condens. Matter 4 8801

(http://iopscience.iop.org/0953-8984/4/45/014)

J. Phys.: Condens. Matter 4 (1992) 8801–8812. Printed in the UK

Energy transfer processes observed in the scintillation decay of BaF_2:La

R Visser†, P Dorenbos†, C W E van Eijk† and H W den Hartog‡

† Radiation Technology Group, Department of Applied Physics, Delft University of Technology, Mekelweg 15, 2629 JB Delft, The Netherlands

‡ Solid State Physics Laboratory, State University of Groningen, Nijenborgh 18, 9747 AG Groningen, The Netherlands

Received 27 May 1992, in final form 1 September 1992

Abstract. The luminescence decay of BaF_2 doped with lanthanum was studied. The decay shows contributions from cross-luminescence (CL) and self-trapped exciton (STE) luminescence. The STE luminescence is quenched in the doped crystals, and shows two non-exponential decay components. Models yielding good fits to the decay data are discussed, as well as the physical relevance of the fitting parameters found.

1. Introduction

BaF_2 is known as the fastest solid state scintillator for gamma ray detection purposes. This is due to the well known cross-luminescence (CL) bands at 195 nm and 220 nm [1–5]. Besides the fast luminescence, BaF_2 shows a much slower luminescence from self-trapped excitons (STEs) having a decay time of 620 ns [2]. This is undesirable for fast scintillation techniques. The slow luminescence component can be reduced by lanthanum doping [6], but the mechanism of this quenching has not been studied in detail. In order to elucidate this mechanism and gain insight into the kinetics of the STE luminescence we undertook the present study.

In this paper, we interpret the kinetics of the STE luminescence in terms of the following processes. After absorption in a BaF_2 crystal of a 662 keV gamma quantum from a ^{137}Cs source, within picoseconds a cloud of hot free electrons and holes is created. These hot charge carriers can diffuse during a short time and then become trapped. Several experiments described in [7] showed that the self-trapping time is less than some tens of picoseconds in the alkali halides. In BaF_2 an analogous value may be expected.

A hole can be self-trapped at two neighbouring fluorine ions, forming an F_2^- centre along one of the basis vectors of the unit cell. This configuration is usually called a V_K centre. Self-trapping of electrons is less likely because the conduction band is much broader than the valence band and the bond strength of Ba_2^{3+} is less than that of F_2^- [7]. However, an electron can be captured at an electron trapping centre, e.g. at a fluorine vacancy (F-centre), or at a self-trapped hole. In the latter case an STE is formed. Remaining V_K centres can diffuse through the lattice and find trapped electrons. On encounter, the electron and the hole may form an STE.

Thus, fast ('prompt') STE formation may be expected during the thermalization of electrons and holes, but also formation after an appreciable time when the charge

0953-8984/92/458801+12$07.50

carriers have been (self-) trapped. The STE luminescence might decay exponentially. However, if there are centres in the crystal that can 'absorb' the STE before it has the opportunity to decay by itself, non-exponentially decaying quenched luminescence can result.

2. Experimental procedures

We have measured the luminescence decay of five crystals of BaF_2 doped with LaF_3 at concentrations from 0 up to 6 mol%. The crystals had a cylindrical shape, the 0% crystal being 30 mm in diameter and the other crystals 8 to 10 mm in diameter. The 0% crystal was obtained from Quartz & Silice Holland. It was polished all over. The other crystals were grown in helium atmosphere by means of the Bridgman technique. They were cut perpendicular to the symmetry axis and polished at the top and bottom faces. The optical absorption of the samples was measured using a Hitachi U3200 spectrophotometer or a combination of an ARC VM-502 monochromator and a deuterium or tungsten lamp.

The luminescence decay measurements were based on the single-photon counting technique described by Bollinger and Thomas [8]. The crystal luminescence was excited by 662 keV gamma rays from a ^{137}Cs source. The start and stop signals were measured by two Philips XP2020Q photomultiplier tubes. An adjustable slit or, in the case of wavelength dependent measurements, a monochromator (Jobin Yvon H.10 U.V. with a 1200 grooves mm^{-1} grating) was mounted between the crystal and the stop photomultiplier. If the monochromator was used, a wavelength resolution of 16 nm full width at half maximum (FWHM) was chosen. Data obtained at different time scales of the measuring electronics were linked together. The time resolution of the measurements is about 0.5 ns (FWHM). For calibration of the luminescence intensity, additional pulse height measurements were performed [9]. Simulation of the pulse height measurements using the shape of the luminescence decay yielded the absolute intensity of the luminescence in terms of the number of photons emitted from the crystal per unit time and per MeV of absorbed excitation energy. All measurements were performed at room temperature.

3. Results

We performed absorption measurements in order to get an idea of the possible STE luminescence quenching centres present in the BaF_2:La crystals. This will be described in subsection 3.1. In subsection 3.2 we will present the observed decay of the luminescence and isolate the contributions to the luminescence from CL and STE luminescence.

3.1. Absorption data

Figure 1 shows the absorption of a 1.3 mol% doped sample. T is the optical transmission. The maximal value was $T_{max} = 0.92$, and not 1. This is mainly due to Fresnel reflections at the crystal surface. The absorption measurements were performed directly after growth and also at the time we did the decay measurements reported in this paper. In the figure, one observes a structureless absorption component increasing for shorter wavelengths. Within error, this was the same for all

samples, irrespective of their lanthanum concentration and thickness. It is attributed to (wavelength-dependent) Fresnel reflection and/or surface impurities. The 15 nm broad absorption band at 290 nm in curve a is attributed to a concentration of 1×10^{22} m^{-3} of cerium. The origin of the 70 nm broad band near the same wavelength in curve b is not clear, but it could be related to x-ray induced radiation damage. The absorption spectra of other samples were comparable to those in figure 1. Roughly, in the wavelength region shown, the absorption coefficients of the 0%, 0.2%, 0.5%, 1.3% and 6% doped samples are proportional to 1.0, 2.0, 1.7, 2.5, and 3.6 respectively.

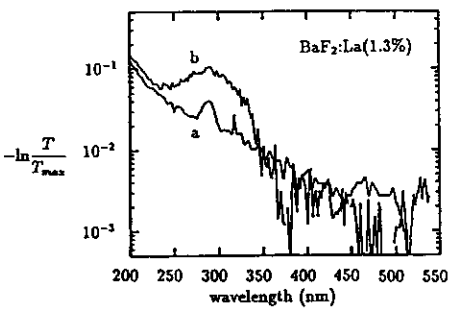

Figure 1. Optical absorption $-\ln(T/T_{max})$ of 3.24 mm thick BaF_2 doped with 1.3 mol% of lanthanum. (a) Directly after growth and polishing; (b) at the time the liminescence decay measurements were performed.

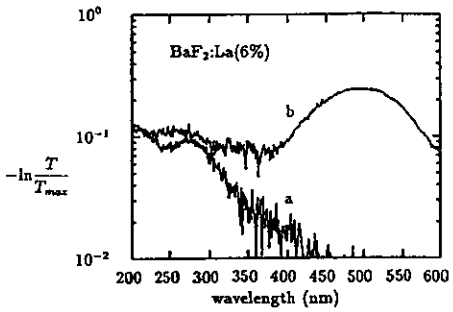

Figure 2. $-\ln(T/T_{max})$ for the 5.1 mm thick BaF_2:La(6 mol%) sample (a) before and (b) after x-irradiation.

After x-irradiation, the lanthanum doped crystals were coloured light pink. The coloration extended down to about 0.6 mm below the surface of the crystal, which is due to the limited penetration depth of the x-rays. The coloration was not observed in the undoped crystal and it increased with lanthanum doping. For the 6 mol% doped BaF_2 crystal we measured the absorption spectrum after 1100 seconds of irradiation of the crystal surface using an x-ray tube with copper anode operated at 35 kV. From the geometry used, the surface irradiation dose was estimated to be $6 \times 10^{15.0 \pm 0.3}$ MeV m^{-2}. The absorption spectrum measured 30 minutes after the irradiation is shown in figure 2, together with the absorption before irradiation. It is seen that the irradiation has given rise to a broad absorption band centred near 500 nm. In BaF_2 doped with 0.01 wt% of trivalent rare earth impurities (except for Sm and Eu) a similar band was observed by Vakhidov *et al* [10] at 77 K after gamma irradiation.

If the crystals were kept in the dark, the absorption band discussed above lasted a few days at room temperature. Illuminating the crystals with a tungsten lamp (distance 2 cm) operated at 22 W input power, which emits light with wavelengths larger than 250 nm, caused bleaching of the band within one minute. All luminescence decay measurements described below were performed with uncoloured crystals.

3.2. The decay of the STE luminescence

The decay of the luminescence of the BaF_2:La samples is shown in figure 3. The unit 'phe/(MeV ns)' denotes the number of photoelectrons from the photomultiplier

photocathode detected during the pulse-height measurements [9], per MeV of absorbed gamma ray energy and per ns of luminescence time. To convert this to the number of photons emitted from the crystal per MeV ns, one can use the relation 1 phe = (6 ± 1) photons. The luminescence decay was measured without wavelength discrimination and with air between the sample and the stop photomultiplier. Thus, figure 3 shows the luminescence decay, integrated over the wavelength interval from 180 nm (the absorption edge of air) to about 600 nm (the cut-off of the photomultiplier). The data are not corrected for the wavelength dependence of the detection efficiency of the photomultiplier. The replica of the luminescence near $t = 0$, which is seen at 15 ns, is an artefact which is due to the electronics.

Some main features are evident in figure 3. At short times the luminescence is dominated by an exponential decay with a decay time of somewhat less than one nanosecond. This is the well known fast CL decay component of BaF_2 [1–5]. At intermediate times, up to about 3 μs, an exponential-like decay is observed, due to the STE luminescence. At long times, we observe a power-law-like decay, which to our knowledge has not been reported so far for BaF_2. The intermediate and long-time behaviour are separated by a 'kink' in the curves near 3 μs, which is most pronounced in the more heavily doped samples.

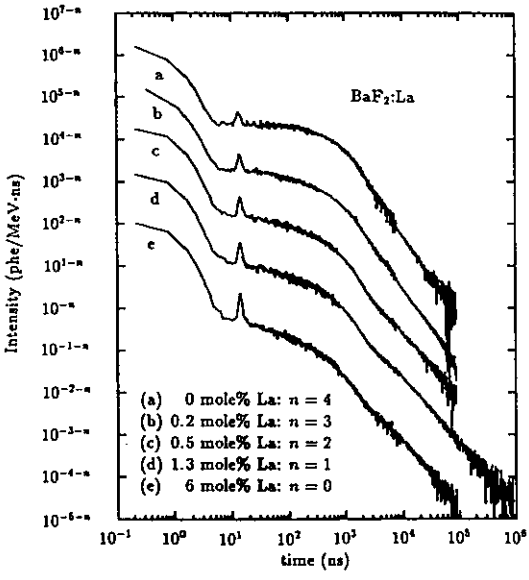

Figure 3. Luminescence decay of the 5 to 7 mm thick BaF_2:La samples, measured wavelength independently. The peak replica at 15 ns belonging to the main peak at $t = 0$ is an artefact.

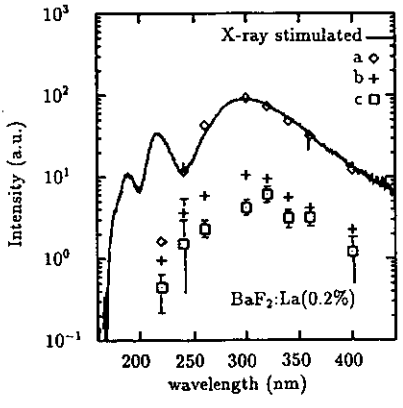

Figure 4. The luminescence intensity (photon output per unit wavelength) of BaF_2:La(0.2 mol%) in the time intervals (a) (0.7 μs, 1.7 μs), (b) (4 μs, 7 μs), and (c) (7 μs, 13 μs) after absorption of a ^{137}Cs gamma photon, as a function of the emission wavelength. For points without error bar, the error is of the order of the point size. The curves are on the same vertical scale. The time-averaged x-ray induced luminescence is also shown and displaced vertically. Corrections have been made for the wavelength dependence of the detection efficiency.

In order to determine the origin of the power-law-like decay component, the luminescence intensity integrated over several time intervals in the microsecond range after absorption of a ^{137}Cs gamma quantum was measured as a function of wavelength. The time intervals chosen are (0.7 μs,1.7 μs), (4 μs, 7 μs), and (7 μs, 13 μs). Beyond 13 μs the signal disappeared in the (statistical) noise. Results of these measurements are shown in figure 4 for the 0.2 mol% doped sample. Also shown is the x-ray-excited emission spectrum, time integrated, showing the well known STE band at 300 nm and the CL bands peaking at 195 nm and 220 nm. It is seen that within error the spectral shape of the luminescence at the three time intervals follows the STE band. For the (0.7 μs, 1.7 μs) interval this is mainly due to the intermediate time component of figure 3. Instead, for the other two time intervals this component is negligible and the long-time component is predominant. Thus, figure 4 suggests that both components are due to STE decay.

At times shorter than 7 ns, and also in the replica region near 15 ns, the sub-nanosecond CL obscures the behaviour of the STE luminescence. In order to isolate the STE luminescence from the CL, the latter had to be suppressed. This was done by recording the luminescence decay at 365 nm. An example of the measured decay is shown in figure 5 for the 6% doped sample. The ordinate shows the number of registered events per μs of measurement time range, per second of measuring time. For correction purposes we also measured the luminescence decay under identical experimental conditions but without a crystal. This resulted in a curve also shown in figure 5, which is due to Cherenkov light caused by fast gamma-excited free electrons in the glass and the fused silica of the start photomultiplier. The figure shows that the Cherenkov light does not seriously affect the recorded data.

The luminescence decay shown in figure 5 shows that at 365 nm some CL is present. Therefore, we also recorded the luminescence decay at 220 nm, which is entirely due to CL. In all samples, within experimental error this CL decay curve was a simple exponential with a 1/e decay time of 0.86 ± 0.04 ns, consistent with earlier observations [5,6]. We multiplied this CL decay curve with a factor and subtracted it from the luminescence decay observed at 365 nm. The multiplication factor was chosen such that the remaining curve was smooth. This decay curve is denoted 'corrected' in figure 5.

Results similar to those of figure 5 are obtained for the other crystals. The multiplication factors of the 220 nm luminescence, necessary to obtain a smooth curve, turned out to be the same for all samples and equal to $(6 \pm 3) \times 10^{-3}$. At 300 nm the CL component was about a factor 3 higher than at 365 nm. Apart from this more intense CL, the luminescence decay shape at 300 nm showed no difference from that at 365 nm, which Kubota *et al* also found for pure BaF_2 [5]. This means that the 'corrected' decay at 365 nm has the same shape as the wavelength-integrated STE luminescence decay. Fitting the smooth 'corrected' curves like that of figure 5 to the curves of figure 3 thus yielded the decay of the STE luminescence. This is shown in figure 6.

4. Interpretation of the data

In the introduction, we noted that STEs can be formed at different times after the absorption of a gamma quantum. Also an STE, when formed, can decay radiatively, but non-radiatively as well. In the latter case, quenching centres may be involved.

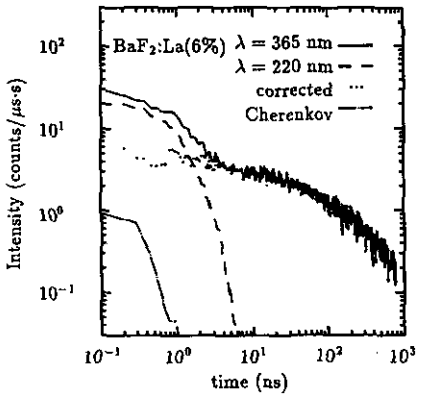

Figure 5. Luminescence decay of the BaF_2:La (6 mol%) sample, measured at wavelengths λ = 220 nm (multiplied by a scaling factor) and λ = 365 nm. The contribution of Cherenkov light is shown, as well as the difference between the 220 nm and 365 nm curves ('corrected').

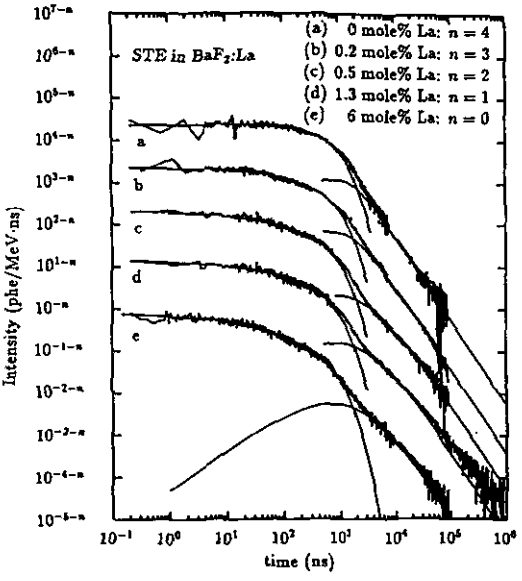

Figure 6. The decay of STE luminescence from BaF_2:La samples. The drawn curves are fits to the data according to table 1 and table 3.

Therefore, we write the STE luminescence decay as:

$$L(t) = I(t) * \frac{1}{\tau_r} \exp[-t/\tau - H(t)] \tag{1}$$

$L(t)$ is the rate at which STE luminescence photons are emitted after the absorption of a gamma quantum at time $t = 0$. $I(t)$ is the rate at which STEs are formed, $1/\tau_r$ is the radiative STE decay rate, and τ is the 1/e decay time of the STE in pure BaF_2. We have $1/\tau = 1/\tau_r + 1/\tau_{nr}$, where $1/\tau_{nr}$ is the rate at which the isolated STE decays non-radiatively, due to internal thermal quenching. $H(t)$ is a function describing non-radiative decay of the STE due to other centres in the crystal. The symbol $*$ denotes the convolution defined by

$$f(t) * g(t) \equiv \int_0^t \mathrm{d}t'\, f(t')g(t-t'). \tag{2}$$

First we focus on the first convolution factor in equation (1), i.e. $I(t)$. The creation of STEs may be very fast, from hot electrons and holes. It may also be slower, if electrons and holes are (self-) trapped before forming an STE. For the latter process, we used the theory of Waite [11]. According to this theory, the concentration of electrons and holes is given by

$$\mathrm{d}n_h/\mathrm{d}t = -4\pi r_{m1} D\left(1 + r_{m1}/\sqrt{\pi Dt}\right) n_h^2. \tag{3}$$

Here we put the concentration of electrons equal to the concentration $n_h(t)$ of holes. As soon as a hole and an electron approach each other to within the minimal distance r_{m1}, they react and form an STE. The subscript '1' is added to distinguish the quantity from r_{m2}, which will be introduced later. $D = D_h + D_e$ is the sum of the electron and hole diffusion constants. From the above, we arrive at the following expression for the STE creation rate $I(t)$:

$$I(t) = N_{STE}(0)\,\delta(t) + N_h(0)\,4\pi r_{m1} D n_h(0)\left[1 + \frac{r_{m1}}{\sqrt{\pi D t}}\right] \times \left[1 + 4\pi r_{m1} D n_h(0)\left(t + 2\frac{r_{m1}}{\sqrt{\pi D}}\sqrt{t}\right)\right]^{-2}. \quad (4)$$

The first term represents the instantaneous formation of the number $N_{STE}(0)$ of STEs at time $t = 0$. This accounts for the fast recombination of hot electrons and holes within the first picoseconds. The second term represents STE formation at later times, and equals $-(d/dt)N_h(t)$. Here $N_h(t) = \int d^3r\, n_h(r,t)$, i.e. the total number of holes in the crystal. $n_h(t)$ is the average of $n_h(r,t)$ over the positions r within the volume that is excited by the gamma ray.

Now we turn to the second convolution factor in equation (1). The STE luminescence in pure BaF_2 can be enhanced by a factor 2.2 ± 0.2 by lowering the temperature from 294 K to 200 K or lower [12]. This suggests that at room temperature, $\tau_r = (2.2 \pm 0.2)\,\tau$. Further, we put $H(t) \approx \alpha t^{\beta}$ for the moment. This proved to be a reasonable fitting function.

In figure 6 we show fits to the experimental data, using the formalism described above. The contributions from the two terms in $I(t)$ in equation (4) are shown separately. For the pure BaF_2 sample, a good fit to the decay is obtained for $H(t) = 0$. From fitting, we obtain $\tau = 630 \pm 50$ ns. Using the same value of τ for the lanthanum doped samples, good fits are obtained if $\beta \approx \frac{1}{3}$ and the parameter α is chosen optimally for each lanthanum concentration. This determines the exponent in equation (1), leaving $I(t)/\tau_r$ to be fitted. The parameters determining this function are clear from equation (4). They are $N_{STE}(0)/\tau_r$, $N_h(0)/\tau_r$, $4\pi r_{m1} D n_h(0)$, and $r_{m1}/\sqrt{\pi D}$. $N_{STE}(0)/\tau_r$ equals the STE photon emission rate at $t = 0$, due to the instantaneous electron-hole recombination process. The values found for this parameter will be discussed later. The other three parameters all relate to STE formation due to the slow (trapped) electron–hole recombination. The values found for these parameters are shown in table 1 as a function of lanthanum concentration.

Table 1. Fitting parameters determining the long time component of $I(t)$ in BaF_2:La. The parameter $r_{m1}/\sqrt{\pi D}$ was found to be less than 2×10^{-3} $s^{1/2}$ for all La concentrations.

La conc. (mol%)	$4\pi r_{m1} D\, n_h(0)$ (s^{-1})	$N_h(0)/\tau_r$ (phe MeV^{-1} ns^{-1})
0.0	$7 \times 10^{5.0\pm0.2}$	0.55 ± 0.15
0.2	$6 \times 10^{5.0\pm0.2}$	0.60 ± 0.15
0.5	$3 \times 10^{5.0\pm0.2}$	0.40 ± 0.10
1.3	$3 \times 10^{5.0\pm0.2}$	0.30 ± 0.07
6.0	$3 \times 10^{5.0\pm0.2}$	0.18 ± 0.03

Below we will discuss the parameters in table 1. We assume that r_{m1}, D, and τ_r are independent of the lanthanum concentration. Then the parameters $4\pi r_{m1} D n_h(0)$ and $N_h(0)/\tau_r$ both say something about the concentration $n_h(0)$ of holes and electrons. Indeed, the parameters are roughly proportional to each other, as shown in the table. Formally, $n_h(0)$ is the concentration at time $t = 0$, but it may be the concentration at time $t \sim 1$ μs as well, because in the experiment the second term on the right-hand side of equation (4) is only observed well for times $t > 1$ μs.

The parameter $r_{m1}/\sqrt{\pi D}$ was found to be less than 2×10^{-3} $s^{1/2}$. If we assume $r_{m1} = 2$ Å, which seems reasonable due to the localized character of the wavefunctions of the trapped holes and electrons, this means that $D > 3 \times 10^{-15}$ m^2 s^{-1}. Beaumont *et al* [13] have found that the 90° jump frequency of the self-trapped hole in BaF_2 is $\nu = (3.2 \times 10^{12}\ s^{-1}) \exp(-\{0.30 \pm 0.02\ eV\}/k_B T)$. The self-trapped hole diffusion constant can be calculated from this by using the approximate relation $D_h = \frac{1}{3}\lambda^2 \nu$, where D_h is the hole diffusion constant and $\lambda = 2.2$ Å is the distance the hole moves per jump. The result at 294 K is $D_h = 3.6 \times 10^{-13.0 \pm 0.3}$ m^2 s^{-1}. This is larger than the minimum value of D found, which is correct because D is at least D_h.

The above discussion shows that the STE creation may well be due to instantaneous creation and, on a large time scale, to diffusion of trapped electrons and self-trapped holes toward each other. Let us now turn to the function $H(t)$. There are several physical mechanisms which yield $H(t)$ functions that overlap the empirical αt^β ones in the time region of interest. This time region is described approximately by $t/\tau \in (0.01, 1)$. Of the theoretically possible mechanisms, we found that energy transfer by multipole–multipole and exchange interactions can fit the data. In the case of multipole–multipole energy transfer, the interaction rate as a function of the distance r between the STE and the quenching centre is $w_{dd}(r) = (1/\tau_r)(R_0/r)^s$. R_0 is a constant which was calculated by Dexter [14], and s depends on the multipoles involved. For this interaction, $H(t)$ can be written as (see [15, 16] and references therein)

$$H(t) = \tfrac{4}{3}\pi R_0^3 n_A\, \Gamma(1 - 3/s)\, (t/\tau_r)^{3/s}. \tag{5}$$

Here n_A is the concentration of quenching centres (the energy *acceptors*). Equation (5) holds if the minimal possible distance r_{m2} between the STE and the luminescence quenching centre is much less than R_0, which we expect to be so. For $s = 8$ and $s = 10$, this function is approximately proportional to $t^{1/3}$. $s = 8$ holds for dipole–quadrupole interaction and $s = 10$ for quadrupole–quadrupole interaction. Dipole–dipole interaction, for which $s = 6$, did not yield very good fits. The parameters obtained from fitting with multipole–multipole interaction are τ, $\frac{4}{3}\pi R_0^3 n_A (\tau/\tau_r)^{3/s}$, and $N_{STE}(0)/\tau_r$. The second parameter describes the strength of the luminescence quenching, and the third parameter is the initial STE photon emission rate. The values found for these parameters at $s = 8$ and $s = 10$ are shown in table 2.

The assumption that the τ decay time is equal for all samples, led to the fitted value $\tau = 760 \pm 50$ ns, i.e. somewhat larger than the value found for the 0 mol% doped sample if $H(t) = 0$ is assumed. The $N_{STE}(0)/\tau_r$ values in table 2 are proportional to the $N_h(0)/\tau_r$ values in table 1. This could be due to the fact that most trapped holes and electrons at the longer time scales are due to non-radiative dissociation of STEs at shorter times. However, this is speculative. The $\frac{4}{3}\pi R_0^3 n_A (\tau/\tau_r)^{3/s}$ parameter values, which are of order 1, say something about the concentration n_A of STE luminescence quenching centres. In most cases, we have 10 Å $< R_0 <$ 80 Å, resulting

Table 2. Parameters of the fits to the prompt luminescence of figure 6 under the assumption of STE luminescence quenching by multipole–multipole energy transfer. The STE decay time is assumed constant for all La concentrations. The fitted value is $\tau = 760 \pm 50$ ns. The error in $\frac{4}{3}\pi R_0^3 n_A(\tau/\tau_r)^{3/s}$ is 0.1. Also shown is $L/[L]_{n_A=0}$, as calculated from the fitting parameters.

La conc. (mol%)	s	$\frac{4}{3}\pi R_0^3 n_A(\tau/\tau_r)^{3/s}$	$N_{STE}(0)/\tau_r$ (phe MeV^{-1} ns^{-1})	$L/[L]_{n_A=0}$
0.0	8	0.2	2.60 ± 0.10	0.78
	10	0.2	2.60 ± 0.10	0.79
0.2	8	0.8	2.60 ± 0.10	0.39
	10	0.8	2.60 ± 0.10	0.41
0.5	8	1.0	2.00 ± 0.15	0.32
	10	1.2	2.30 ± 0.15	0.27
1.3	8	1.2	1.60 ± 0.20	0.26
	10	1.4	1.80 ± 0.20	0.23
6.0	8	1.6	0.70 ± 0.20	0.18
	10	1.6	0.80 ± 0.20	0.19

in 3×10^{26} $m^{-3} > n_A > 6 \times 10^{23}$ m^{-3}. Considering this, the quenching centre could be related to lanthanum, since the lanthanum concentration is of the order of 1.7×10^{26} m^{-3}, which is one per cent of the barium concentration. However, the $\frac{4}{3}\pi R_0^3 n_A(\tau/\tau_r)^{3/s}$ values are much less than linearly increasing with the lanthanum concentration. This increase follows better the increase of the absorption coefficient as a function of the lanthanum concentration, which was discussed in section 3.1. This suggests that the STE quenching is related to a centre in which lanthanum, as well as another impurity, is involved. The concentration of this impurity would then be less than linearly dependent on the lanthanum concentration. In any case, lanthanum plays a role in the STE luminescence quenching. Considering this, the non-zero value for $\frac{4}{3}\pi R_0^3 n_A(\tau/\tau_r)^{3/s}$ at 0 mol% is somewhat strange, but the deviation from zero is not very large. Even if a small variation of τ for the different samples is allowed, the deviation is not significant.

From the parameters s and $\frac{4}{3}\pi R_0^3 n_A(\tau/\tau_r)^{3/s}$, and equations (1) and (5), we calculated the ratio $L/[L]_{n_A=0} \equiv \int dt\, L(t)/[\int dt\, L(t)]_{n_A=0}$. This is equal to the ratio of the observed STE photon output, and the output which would result if no quenching centres were present ($n_A = 0$), under the condition that the same number of STEs is still created in both cases ($I(t)$ unchanged). This ratio is shown in table 2. The total decrease of the STE photon output is determined by the decrease of the number of STEs created (see the $N_{STE}(0)/\tau_r$ values) and the ratio $L/[L]_{n_A=0}$. As an example, for the 0.5 mol% doped sample and $s = 8$, $N_{STE}(0)/\tau_r$ is 0.77 times its value at 0 mol%, and $L/[L]_{n_A=0} = 0.41$ times its value at 0 mol%. Hence, the STE photon output in this sample is 0.32 times that in the 0 mol% doped sample. This decrease was also observed in the x-ray excited emission spectra. Also for the other samples the decay measurements reported agree quite reasonably with the x-ray-excited emission, which are shown in figure 4 at 294 K in [12]. A comparison of the $N_{STE}(0)/\tau_r$ and $L/[L]_{n_A=0}$ values in table 2 shows that the decrease of the STE photon output is mainly due to quenching centres (especially for low lanthanum concentrations), but also a decrease of the number of created STEs plays a role.

Let us now turn to the other quenching mechanism mentioned above: transfer by exchange interaction. Here, the interaction rate is $w_{exc}(r) = w_0 \exp(-r/r_0)$, where w_0 and r_0 are constants [14]. For this we can write [17,18]

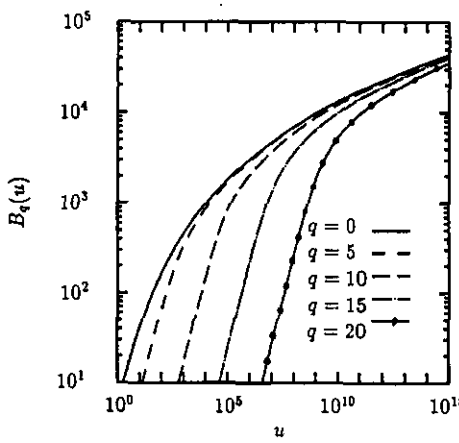

Figure 7. The functions $B_q(u)$ used in equation (6) for $q \in \{0, 5, 10, 15, 20\}$.

$$H(t) = \frac{4}{3}\pi r_0^3 n_A B_q(u) \qquad B_q(u) = \sum_{i=1}^{3} a_i q^{3-i} g_i(ue^{-q}) \tag{6}$$

where

$$a_1 = a_2 = 3 \qquad a_3 = 1 \qquad u = w_0 t \qquad q = \frac{r_{m2}}{r_0}$$

and

$$g_m(x) = m! \sum_{j=1}^{\infty} \frac{(-1)^{j+1} x^j}{j!\, j^m}.$$

Examples of the function $B_q(u)$ are shown in figure 7. r_{m2} is the minimal distance at which the STE and the STE luminescence quenching centre can possibly be. We expect r_{m2} to be about 2 Å and r_0 about 0.5 Å, meaning that $q \sim 4$. It is clear from figure 7 that there is a region of u where $B_4(u)$ is proportional to $u^{1/3}$. In this region, $H(t) \propto t^{1/3}$, so also equation (6) can yield good fits to the STE luminescence decay. The parameters obtained from fitting are shown in table 3. The values for $N_{STE}(0)/\tau_r$ are not much different from those in table 2. The relative variation in the $\frac{4}{3}\pi r_0^3 n_A$ values in table 3 is rather similar to that of the $\frac{4}{3}\pi R_0^3 n_A (\tau/\tau_r)^{3/s}$ values in table 2. Concerning the absolute value of $\frac{4}{3}\pi r_0^3 n_A$, if $r_0 = 0.5$ Å, then table 3 shows that n_A is about 2×10^{27} m^{-3}. This is higher than the values found for multipole–multipole interaction. However, note the uncertainty in this value due to the strong dependence on the precise value of r_0. At 0 mol% we found $\frac{4}{3}\pi r_0^3 n_A = 0$ within error (i.e. $H(t) = 0$). Connected with this is the τ value, which is different from that in table 2. The calculated $L/[L]_{n_A=0}$ values are shown in the last column of table 3. The values differ somewhat from those in table 2, which is due to the difference between the fitted τ values in both tables. The theoretical curves in figure 6 were calculated using the data in tables 1 and 3.

5. Conclusions

In this paper, we presented the decay of the STE in BaF_2:La. The above shows that the values found for the fitting parameters of the model are physically not

Table 3. Parameters of the fits to the prompt luminescence of figure 6 under the assumption of STE luminescence quenching by exchange energy transfer for $r_{m2}/r_0 = 4$. The STE decay time is assumed constant for all La concentrations. The fitted value is $\tau = 630 \pm 50$ ns. $w_0\tau = 4 \times 10^{4.0\pm0.5}$. Also shown is $L/[L]_{n_A=0}$, as calculated from the fitting parameters.

La conc. (mol%)	$\frac{4}{3}\pi r_0^3 n_A$	$N_{STE}(0)/\tau_r$ (phe MeV^{-1} ns^{-1})	$L/[L]_{n_A=0}$
0.0	$< 1.1 \times 10^{-4}$	2.30 ± 0.10	> 0.87
0.2	$5 \times 10^{-4.0\pm0.15}$	2.30 ± 0.10	0.53
0.5	$7 \times 10^{-4.0\pm0.12}$	2.05 ± 0.20	0.42
1.3	$8 \times 10^{-4.0\pm0.13}$	1.40 ± 0.20	0.37
6.0	$1.1 \times 10^{-3.0\pm0.11}$	0.76 ± 0.25	0.27

unrealistic. The quenching of the STE luminescence introduced by the lanthanum doping is mainly due to non-radiative decay of the STE due to some kind of quenching centre present in the crystals. However, a decrease of the number of STEs formed also plays a role, especially at the higher doping levels. The precise nature of the STE luminescence quenching cannot be established, because the data are consistent with different quenching interactions. We note that the La^{3+} ion as such cannot cause any multipole transitions, since the energy needed to excite it is much larger than the energy stored in the STE. However, such processes cannot be excluded for centres like $La^{3+}_{Ba} - O^{2-}_{F}$, in which charge transfer states might be responsible for the quenching of STE luminescence. Such quenching centres, the concentration of which is limited by the amount of oxygen present in the crystal, would be consistent with the fact that the concentration of quenching centres shows only weak dependence on lanthanum concentration. In all samples we observed STE luminescence at times beyond 4 μs, which we assigned to reactions between (self-) trapped electrons and holes yielding STEs on this time scale. From the decay measurements presented it is not possible to conclude which process is responsible for these trapped electrons and holes. For more information on these subjects, additional experiments should be performed.

Acknowledgments

We wish to thank J Th M de Haas for technical assistance during some measurements. These investigations in the program of the Foundation for Fundamental Research on Matter (FOM) have been supported by the Netherlands Technology Foundation (STW).

References

[1] Ershov N N, Zakharov N G and Rodnyi P A 1982 *Opt. Spektrosk.* **53** 89
[2] Laval M, Moszynski M, Allemand R, Cormoreche E, Guinet P, Odru R and Vacher J 1983 *Nucl. Instrum. Methods* **206** 169
[3] Aleksandrov Yu M, Makhov V N, Rodnyi P A, Syreishchikova T I and Yakimenko M N 1984 *Fiz. Tverd. Tela* **26** 2865
[4] Valbis Y A, Rachko Z A and Yansons Y A 1985 *JETP Lett.* **42** 172
[5] Kubota S, Suzuki M, Ruan J, Shiraishi F and Takami Y 1986 *Nucl. Instrum. Methods* A **242** 291
[6] Schotanus P, Dorenbos P, van Eijk C W E and Lamfers H J 1989 *Nucl. Instrum. Methods* A **281** 162

[7] Williams R T and Song K S 1990 *J. Phys. Chem. Sol.* **51** 679 and references therein
[8] Bollinger L M and Thomas G E 1961 *Rev. Sci. Instrum.* **32** 1044
[9] Dorenbos P, Visser R, van Eijk C W E, Hollander R W and den Hartog H W 1991 *Nucl. Instrum. Methods* A **310** 236
[10] Vakhidov Sh A, Kaipov B, Tavshunskii G A and Gapparov N 1976 *Opt. Spektrosk.* **40** 1099
[11] Waite T R 1957 *Phys. Rev.* **107** 463
[12] Dorenbos P, Visser R, Dool R, Andriessen J and van Eijk C W E 1992 Suppression of self-trapped exciton luminescence in La^{3+} and Nd^{3+} doped BaF_2 *J. Phys.: Condens. Matter* **4** 5281
[13] Beaumont J H, Hayes W, Kirk D L and Summers G P 1970 *Proc. R. Soc.*A **315** 69
[14] Dexter D L 1953 *J. Chem. Phys.* **21** 836
[15] Di Bartolo B 1984 *Energy Transfer Processes in Condensed Matter (NATO ASI series)* ed B Di Bartolo and A Karipidou (New York: Plenum) p 103
[16] Rotman S R and Hartmann F X 1988 *Chem. Phys. Lett.* **152** 311
[17] Allinger K and Blumen A 1981 *J. Chem. Phys.* **75** 2762
Note that $e^{\gamma b}$ in equation (3.12) should read $e^{-\gamma b}$
[18] Hartmann F X and Rotman S R 1989 *Chem. Phys. Lett.* **163** 437